

Article

Plot-Scale Runoff Generation and Sediment Loss on Different Forest and Other Land Floors at a Karst Yellow Soil Region in Southwest China

Ruiwen Peng ^{1,2,†}, Han Deng ^{3,†}, Ruoshuang Li ⁴, Yiqiu Li ^{1,2,*}, Guangbin Yang ^{1,2} and Ou Deng ^{1,2}

¹ Karst Institute, School of Geographic and Environments Sciences, Guizhou Normal University, Guiyang 550001, China

² GuiZhou Provincial Key Laboratory of Mountain Resources and Environment Remote Sensing Application, Guiyang 550025, China

³ School of Data Sciences, Fudan University, Shanghai 200000, China

⁴ School of Earth Sciences and Resources, China University of Geosciences, Beijing 100083, China

* Correspondence: 201705002@gznu.edu.cn; Tel.: +86-17385485126

† These authors contributed equally to this work.

Abstract: Yellow soils developed in limestone weathering materials are representative on Guizhou Plateau, Southwest China. As one of the most important cultivated soils in Guizhou Province, karst yellow soils are generally thin and can be significantly damaged by mild soil erosion. This work used the structural equation model (SEM) to analyze the influence of various factors on runoff generation and sediment loss based on a long time series (2015–2020) of natural rainfall-runoff data and soil erosion data collected from 18 runoff plots in the karst yellow soil region of Southwest China, which reflects the erosion dynamics under natural conditions. Slope runoff plots are the most popular and efficient way to collect data on runoff generation and soil erosion. The findings show that: (1) There were 139 rainfall-runoff occurrences between 2015 and 2020, with moderate rain (10–25 mm) and heavy rain (25–50 mm) events making up the majority. Due to its high frequency and prolonged duration, heavy rain had the greatest impact on the overall rainfall erosivity R value (R). (2) Mean surface runoff (SR) values ranged from 17.37 mm to 133.90 mm, while mean sediment loss rates (SLR) ranged from 1.36 t·ha⁻¹·a⁻¹ to 23.49 t·ha⁻¹·a⁻¹. SR and SLR can be successfully reduced by the forest floor. Broadleaf forest, coniferous forest, mixed forest, and orchard had mean SR values of 19.33%, 12.97%, 16.10%, and 33.38% of fallow land, respectively, and had mean SLR values of 6.90%, 5.79%, 6.34%, and 12.64% of fallow land, respectively. (3) SR generation at the plot scale was substantially linked with 30-min maximum rainfall intensity (I₃₀), while vegetation coverage (VC) and antecedent soil water content (ASW) showed negative direct inference on SR and runoff sediment concentration (RSC) according to SEM analysis. The VC and ASW showed the highest indirect impact on SLR. This study will serve as a scientific reference for the water and soil erosion management in karst yellow soil region and serve as a scientific guidance for regional land use in Southwest China.

Keywords: karst area; plot-scale; yellow soil; erosion dynamics; structural equation modeling (SEM)



check for updates

Citation: Peng, R.; Deng, H.; Li, R.; Li, Y.; Yang, G.; Deng, O. Plot-Scale Runoff Generation and Sediment Loss on Different Forest and Other Land Floors at a Karst Yellow Soil Region in Southwest China.

Sustainability **2023**, *15*, 57. <https://doi.org/10.3390/su15010057>

Academic Editors: Zhongke Feng and Zixuan Qiu

Received: 26 October 2022

Revised: 12 December 2022

Accepted: 14 December 2022

Published: 21 December 2022



Copyright: © 2022 by the authors. Licensee MDPI, Basel, Switzerland. This article is an open access article distributed under the terms and conditions of the Creative Commons Attribution (CC BY) license (<https://creativecommons.org/licenses/by/4.0/>).

1. Introduction

The global karst regions cover 2.20×10^7 km² of which 5.10×10^6 km² are exposed to the Earth's surface and account for about 12% of the Earth's surface [1–3]. Drinking water from karst aquifers is a necessity for about 25% of the world's population [4].

China's karst region covers 3.44×10^6 km² and accounts for about 1/3 of the national territory [1,2,5]. One of the largest continuous karst terrain areas in the world exposed to a subtropical environment is in China's southwest. It has an area of 51.97×10^4 km² [1]. Karst mountains, which make up roughly 73% of the karst area and have many slopes and valleys, dominate a significant portion of the karst terrain [1].

For runoff generation and groundwater recharge, karst mountains are a crucial type of landscape unit [6,7]. The mountains have seen serious environmental deterioration, including loss of forest cover, erosion of the soil, extinction of wildlife, and frequent catastrophic droughts and floods [8,9]. On sites with limestone bedrock underlain, runoff generation and soil erosion dynamics have been found to be particularly complex [10]. Limestone bedrocks could be easily weathered and transform into yellow soil in the karst region. As a crucial part of the earth's system, soil regulates the cycles of hydrology, erosion, geochemistry, biology, and ecology and is also an important source of resources, goods, and services for humanity [11]. However, due to the intrinsic detrimental properties of soil production and environmental harm, increased soil erosion poses a threat to human societies [12–16].

Both theory and practice might benefit from a deeper comprehension of soil erosion mechanisms. Slope runoff plots are a common facility for runoff generation and sediment loss monitoring and are the most widely used and effective method for obtaining soil erosion data [17,18]. Runoff plots have been used in numerous countries throughout the past century to estimate surface runoff and sediment loss rates [19–22]. The first runoff plots were built by Miller (1926) in Missouri, USA [23]. Studies of runoff generation and sediment loss are frequently conducted on bounded plots from which runoff and sediment loss are monitored following each rainfall event [24–27]. Extensive analyses of soil loss over vast areas have also been carried out in various countries or continents by adopting field-measured data from runoff plots.

Both the widely used universal soil loss equation (USLE) and the revised universal soil loss equation (RUSLE) were developed using runoff plots and field-measured data collected over an extended period of time [24,28,29]. On the basis of data collected from runoff plots in the field, a number of local erosion assessment models have also been created for Europe [30,31], Africa [32,33], Australia [34], and China [18,35,36]. The basic magnitude of soil erosion for various nations or continents was provided by these data.

Plots runoff generation and sediment loss research in China has a long history. In China, field measurements first began in 1922. To investigate the impacts of forest vegetation on soil erosion, runoff plots were built in Qinyuan, Ningwu, and Qingdao, Shanxi Province with the assistance of the American scientist, W.C. Lowdermilk [37]. Runoff plots have been used in a variety of experimental investigations over the past 90 years in China that have yielded important data on the country's runoff and sediment loss rates [38–41]. These studies investigated the variability of both runoff generation and sediment loss rates in addition to providing a foundation for understanding the mechanisms of runoff generation and sediment loss among different regions, land uses, soils, and vegetation types.

The majority of these studies focused on the connection between vegetation type and runoff process and mainly used short-term rainfall modeling experiments [22,42–44]. A prominent problem in geosciences and ecology has only recently come to light in a few studies that the influence of vegetation on the runoff process and features is connected to the kind, quantity, and geographic distribution of vegetation [45,46].

As one of the most important cultivated soils in Guizhou Province, Southwest China, karst yellow soil is generally thin and can cause significant damage by mild soil erosion [47,48]. Karst landscapes and yellow soils have a high geospatial overlap. Yellow soils developed in limestone weathering materials are representative on the Guizhou Plateau, and the distribution area of yellow soils accounts for about 46.50% of the area of Guizhou province of which 55.95% are distributed in karst areas. The studies of runoff generation and sediment loss in the Guizhou karst region started relatively late [49], among which few studies had dealt with the karst yellow soil erosion [48]. Previous studies discussed the soil erosion influencing factors [50], the flow and sand production characteristics [25,51], the erosive rainfall criteria, and rainfall erosivity [48,52], which provided a good research basis and research reference for this study.

In this work, natural rainfall-runoff data from 18 runoff plots on a karst hillslope in Longli County in the karst yellow soil region of Guizhou Province, Southwest China were gathered over a lengthy period of six years (2015–2020) to investigate the peculiarities of the natural rainfall in the region and its connection with soil erosion. Monitored parameters include precipitation (P , mm), 30-min maximum rainfall intensities (I_{30} , mm/h), antecedent soil water content (ASW, %), vegetation coverage (VC, %), surface runoff (SR, mm), runoff sediment concentration (RSC, $\text{kg}\cdot\text{m}^{-3}$), sediment loss rate (SLR), and rainfall erosivity R value (R , $\text{MJ}\cdot\text{mm}/(\text{ha}\cdot\text{h})$). The variability of runoff generation and sediment loss on different forest and other land floors under natural rainfall conditions are thoroughly discussed considering both the direct and indirect factors to determine the internal relationship of nature rainfall, runoff generation, and sediment loss of the karst yellow soil region and to evaluate the effects of different water conservation measures to reduce the runoff generation and sediment loss. This study will serve as a scientific reference for the water and soil erosion control in the Southwest Chinese karst yellow soil region and provide comprehensive suggestions for scientific land use management.

2. Materials and Methods

2.1. Experimental Site Description

This study was conducted in Yangjichong small catchments which belong to the Wujiang river system of Yangtze River basin located in the eastern part of Longli County. Longli County is approximately 35 km southeast of Guiyang, Guizhou Province, Southwest China (Figure 1). The altitude ranges from 770 m to 1775 m. The soils are of mountain yellow loam and are sensitive to erosion. The center position is located at $107^{\circ}00'53''$ E and $26^{\circ}26'58''$ N, and it belongs to the northern subtropical monsoon humid climate area. The long-term average annual temperature in this region is 14.8°C and annual rainfall is about 1100 mm [50]. Although there are significant changes in some locations due to the extensive terrain undulations, the climate is generally pleasant as a result of the influence of the high latitude, which is warm in winter and cool in summer.

2.2. Methodological Approach

(1) Experimental plots under natural rainfall data collection

In the Yangjichong soil and water conservation monitoring station, 18 runoff plots with various plating patterns were established to quantify land surface runoff generation and sediment loss. The plots were divided into seven groups by land cover type: two broadleaf forest plots (S1–S2), two coniferous forest plots (S3–S4), two mixed forest plots (S5–S6), two farmland plots (S7–S8), two natural grassland plots (S9–S10), two fallow plots (S11–S12), and six orchard plots (S13–S18). The runoff plots distribution map is shown in the following Figure 2.

Twelve forest runoff plots (S1–S6 and S13–S18) were established along the slope of 20° with dimensions of 20×5 m and 20×9 m under canopies of different species. The plots, S1–S6, are water conservation forests, including broadleaf forest (poplar), coniferous forest (cypress), and mixed forest (poplar and cypress). The plots, S13–S18, are orchard economic forests with waxberry, peach, pear, and raspberry, respectively. Two cropland runoff plots of S7–S8, with dimensions of 15×5 m, were installed along the slope of 20° in a shrubby area. Two natural grassland plots (S9–S10) and two fallow plots (S11–S12) were established along the slope of 25° with dimensions of 20×5 m (Table 1). Stainless steel troughs were erected parallel to the slope contour at the lowest edge of these plots. All these plots with different vegetation types and water conservation measures quantify the effect of direct and indirect relationships on surface runoff (SR) and sediments loss rate (SLR).

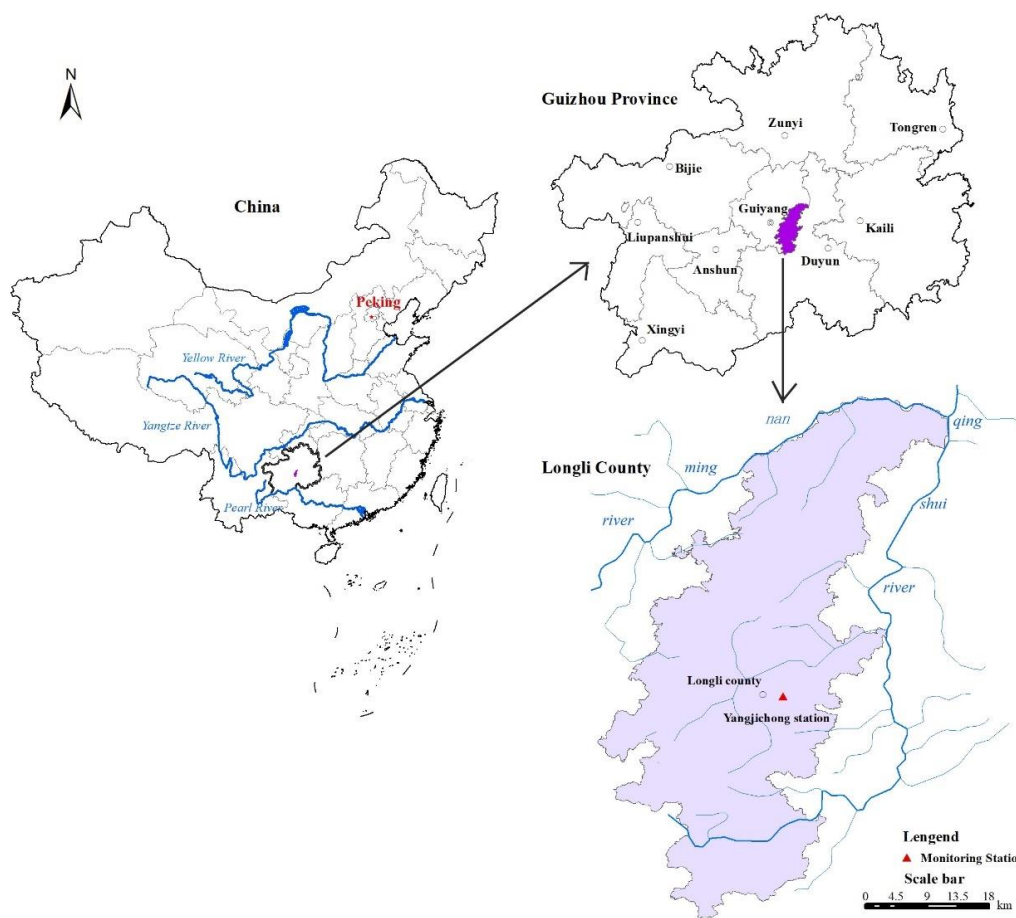


Figure 1. Location of Yangjichong monitoring station.

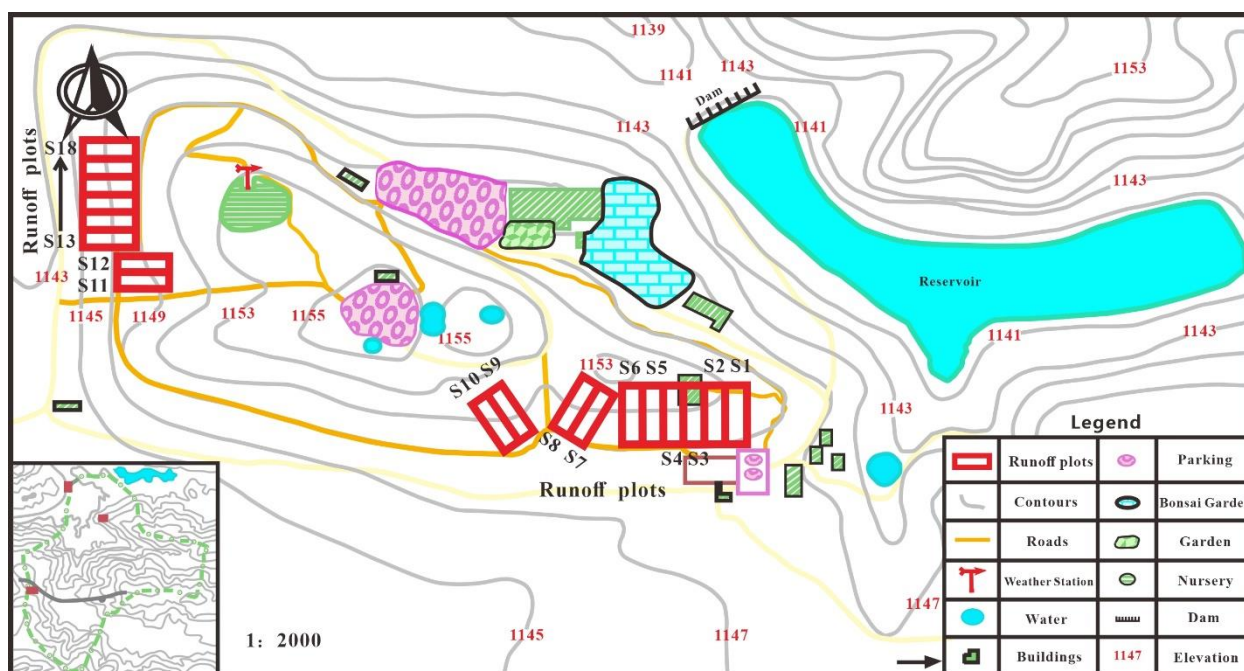


Figure 2. Location of the runoff plots. The runoff plots numbers, S1–S18, are marked on the side; different colors represent different land cover types.

Table 1. Basic information table of runoff plots.

Plots	Bedrock Types	Soil Types	Slope/Degree	Plot Size/Width × Length, m	Vegetation Types	Species
S1–S2	Limestone	Yellow soil	20.0	20.0 × 5.0	Broadleaf forest	Poplar
S3–S4	Limestone	Yellow soil	20.0	20.0 × 5.0	Coniferous forest	Cypress
S5–S6	Limestone	Yellow soil	20.0	20.0 × 5.0	Mixed forest	Poplar and cypress
S7–S8	Limestone	Yellow soil	25.0	20.0 × 5.0	Cropland	Corn, green vegetables
S9–S10	Limestone	Yellow soil	25.0	20.0 × 5.0	Grassland	Natural meadow
S11–S12	Limestone	Yellow soil	25.0	20.0 × 5.0	Fallow	bare
S13–S18	Limestone	Yellow soil	20.0	18.0 × 10.0	Orchard	Waxberry, peach tree, pear tree, raspberry

(2) Data Acquisition and Processing

The HOBO small automatic weather station was used to monitor the data. Rainfall was observed on time at 8:00 a.m. every day by HOBO JII siphon type self-recording rain gauge (Onset, Cape Cod, MA, USA), and the operation of the instrument was inspected at 20:00 on the day of precipitation, and the number of inspections was increased appropriately during heavy rainfall to find and troubleshoot in time and prevent missing the rainfall process.

Monitoring indicators included rainfall order, rainfall time, cumulative rainfall (mm), cumulative duration (min), rainfall amount (mm), duration (min), rain intensity (mm/h), etc. The rainfall process was excerpted at 5 min intervals, and the rainfall intervals greater than 360 min were recorded as two rainfalls [53]. Surface runoff (SR, mm) and runoff sediment concentration (RSC, $\text{kg}\cdot\text{m}^{-3}$) were manually sampled after each flow production by measuring runoff depth of the diversion pool and sediment content of collection pool (two samples for each runoff plot when mixing evenly).

(3) Calculations and statistical analysis

(1) Rainfall characteristics analysis. Based on the 5-min intervals rainfall process data, 30-min maximum rainfall intensities (I_{30} , mm/h) and rainfall erosivity R value (R , $\text{MJ}\cdot\text{mm}/(\text{ha}\cdot\text{h})$) were calculated. The 30-min maximum rainfall intensity was the maximum value of the sum of rainfall in any 30-min period during the rainfall process and then divided by 0.5 and converted into mm/h. The rainfall erosivity R value was determined using the method provided by Wischmeier [54]:

$$R = EI_{30} \quad (1)$$

$$E = \sum_{r=1}^n (e_r \cdot p_r) \quad (2)$$

$$e_r = 0.29[1 - 0.72 \exp(-0.082i_r)] \quad (3)$$

where R is the rainfall erosivity R value ($\text{MJ}\cdot\text{mm}/(\text{ha}\cdot\text{h})$), I_{30} is the 30-min maximum rainfall intensity (mm/h), E is the total kinetic energy of a rainfall (MJ/ha), $r = 1, 2, \dots, n$ is a rainfall process divided into n periods according to rainfall intensity, P_r is the r -th period rainfall (mm), e_r is the unit rainfall kinetic energy for each time period ($\text{MJ}/\text{ha}\cdot\text{mm}$), i_r is the r -th period rainfall intensity (mm/h).

(2) Effecting factors analysis. Structural equation modeling (SEM) is a method for building, estimating, and testing causality models [55]. The application of SEM is increasing in the fields of ecology, forestry engineering, and soil and water conservation [56,57]. The traditional SEM path analysis was adopted in this paper where all variables of the model were measured indicator variables and is called path analysis with observed variables (PA-OV model). In this study, the SEM was used to evaluate both the direct and indirect relationships among precipitation (P , mm), 30-min maximum rainfall intensity (I_{30} , $\text{mm}\cdot\text{h}^{-1}$), rainfall erosivity R value (R , $\text{MJ}\cdot\text{mm}\cdot\text{ha}^{-1}\cdot\text{h}^{-1}$), surface runoff (SR, mm), antecedent soil water content (ASW, %), vegetation coverage (VC, %), runoff sediment

concentration (RSC, $\text{kg}\cdot\text{m}^{-3}$), and sediments loss rate (SLR). Using p -values, chi-squared values, the goodness-of-fit index, and the root mean square error of approximation, the fit of the structural equation modeling (SEM) was assessed. The Amos 24.0 software program developed by Amos Development Corporation, Chicago, IL, USA was used for the SEM, and unless otherwise stated, results were deemed significant when $p < 0.05$ [58,59].

3. Results

3.1. Rainfall and Rainfall-Runoff Events Characteristics

The annual rainfall amounts from 2015 to 2020 were 1260.9 mm, 1025.8 mm, 1137.9 mm, 1206.0 mm, 1238.0 mm, and 1377.3 mm, respectively. The average annual rainfall is 1207.7 mm, higher than the long-time average annual rainfall of 1100 mm. The daily rainfall amount of 2015–2020 is shown in Figure 3. Rainfall days were more than 140 days in each year, and over 80% of the rainfall were concentrated in April–October (Figure 3).

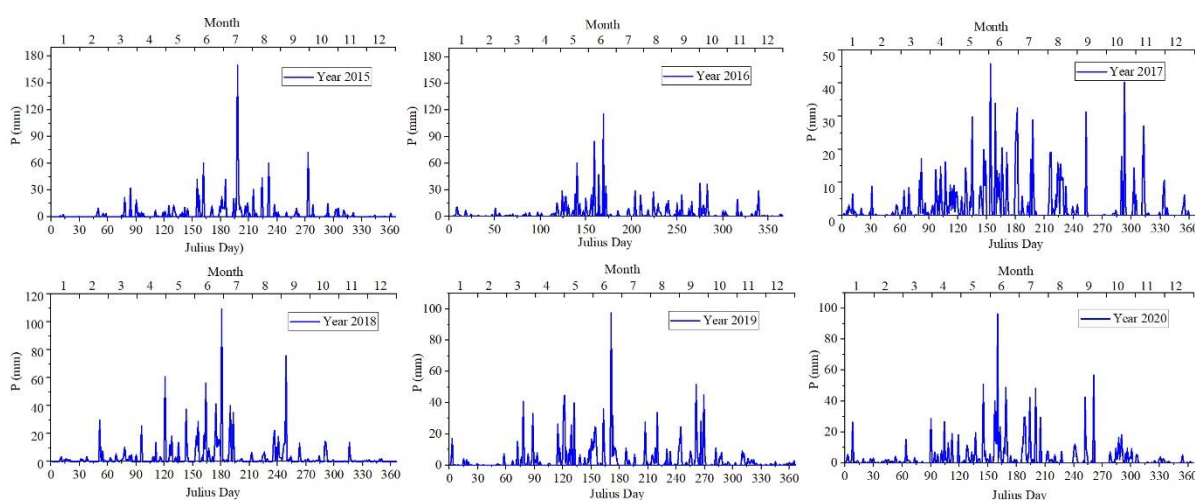


Figure 3. Daily rainfall amounts for 2015–2020.

Between 2015 and 2020, 325 rainfall events ranging between 15 min and 24 h and measuring more than 5 mm within a typical 6-h span were recorded. If rainfall was not measured for more than 6 h, it was classified as two rainfall occurrences and counted toward the standard 6-h interval. Of all these 325 rainfall events, there were 139 rainfall-runoff events occurring in 2015–2020. Properties, such as precipitation (P , mm), 30-min maximum rainfall intensities (I_{30} , $\text{mm}\cdot\text{h}^{-1}$), and rainfall erosivity R value (R , $\text{MJ}\cdot\text{mm}\cdot\text{ha}^{-1}\cdot\text{h}^{-1}$) of these rainfall-runoff events in 2015–2020 are shown in Figure 4.

The rainfall-runoff events occurring during 2015–2020 were 27, 24, 22, 23, 23, and 20 in each year, respectively. The total rainfall from the annual rainfall-runoff event is the annual erosive rainfall, and the annual erosive rainfall from 2015 to 2020 were 823.6 mm, 628.2 mm, 731.4 mm, 796.6 mm, 781.1 mm, and 737.6 mm, respectively. The rainfall-runoff events generated gross rainfall amounts ranging from 9.6 to 116.8 mm with 30-min maximum rainfall intensities ranging from 3.23 to 89.6 $\text{mm}\cdot\text{h}^{-1}$.

The 24 h rainfall is divided into six levels: light rain (≤ 10 mm); moderate rain (10–25 mm); heavy rain (25–50 mm); rainstorm (50–100 mm); heavy rainstorm (100–250 mm); and very heavy rainstorm (≥ 250 mm) [60]. Moderate rain and heavy rain events were the main rainfall-runoff events, which occurred 62 times and 58 times, respectively. Heavy rain contributed the most to the total rainfall erosivity R value because of its high frequency and long duration. The heavy rainfall did not occur frequently, but the rainfall erosivity of a single heavy rainfall can be very large.

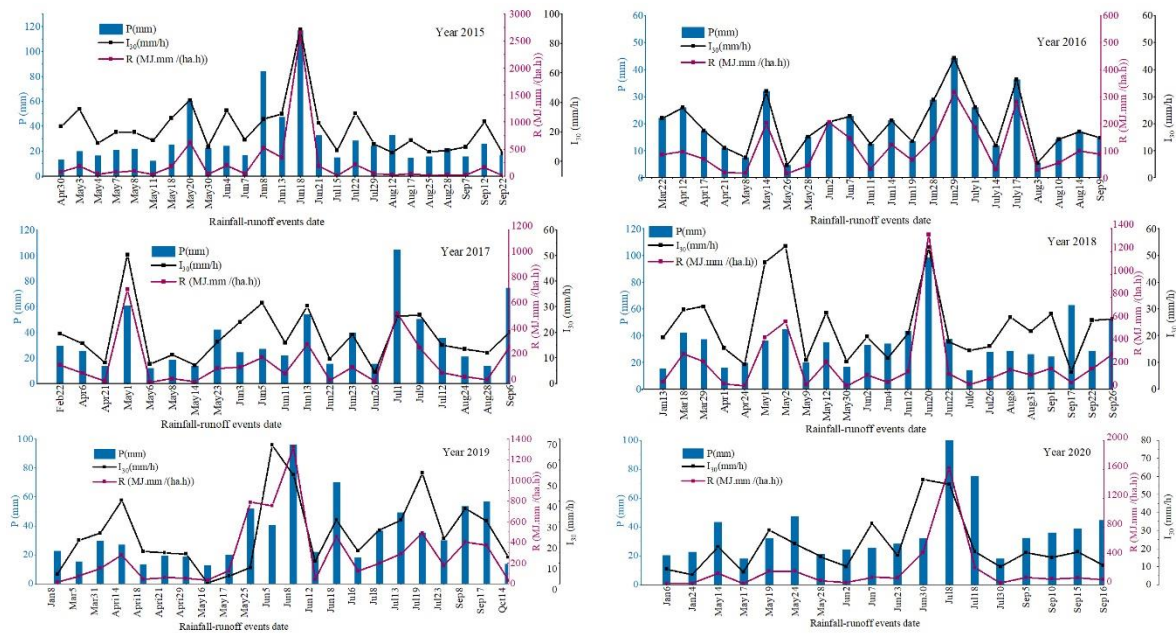


Figure 4. Properties of rainfall-runoff events in 2015–2020. Note: the color of the coordinate axes corresponds to the color of lines and columns. Blue: precipitation (P, mm); black: 30-min maximum rainfall intensities (I_{30} , $\text{mm}\cdot\text{h}^{-1}$); purple: rainfall erosivity R value (R , $\text{MJ}\cdot\text{mm}\cdot\text{ha}^{-1}\cdot\text{h}^{-1}$).

The maximum rainfall-runoff event with the rainfall of 116.8 mm emerged on 18 June 2015, and its 30-min rainfall intensity was also the largest, $89.6 \text{ mm}\cdot\text{h}^{-1}$, as mentioned above. The rainfall erosivity R value of the rainfall-runoff events ranged from 6.16 to $2661.13 \text{ MJ}\cdot\text{mm}\cdot\text{ha}^{-1}\cdot\text{h}^{-1}$; the highest rainfall erosivity R value of $2661.13 \text{ MJ}\cdot\text{mm}\cdot\text{ha}^{-1}\cdot\text{h}^{-1}$ also emerged on 18 June 2015.

3.2. Plot Runoff Amounts and Sediment Concentration Characteristics

(1) Surface runoff characteristics

The surface runoff (SR, mm) of all the 139 rainfall-runoff events in 2015–2020 are shown according to the 18 runoff plots in Figure 5.

As previously mentioned, the 18 plots were divided into seven groups. The surface runoff (SR, mm) and runoff coefficient (RC, %) statistical parameters, such as mean value and standard deviation (SD), of the seven groups plots are listed in the following Table 2.

Table 2. The surface runoff and runoff coefficients of runoff plots.

Plots	Vegetation Types	SR (mm)		RC (%)	
		Mean	SD	Mean	SD
S1–S2	Broad-leaved forest	25.88	6.07	3.48	3.36
S3–S4	Coniferous forest	17.37	6.48	2.31	7.63
S5–S6	Coniferous and broad-leaved mixed forest	21.56	6.09	2.85	6.36
S7–S8	Cropland	82.89	23.81	10.97	26.05
S9–S10	Grassland	44.69	6.95	6.01	6.15
S11–S12	Fallow	133.90	30.31	17.77	31.98
S13–S18	Orchard	37.03	6.04	4.98	4.87

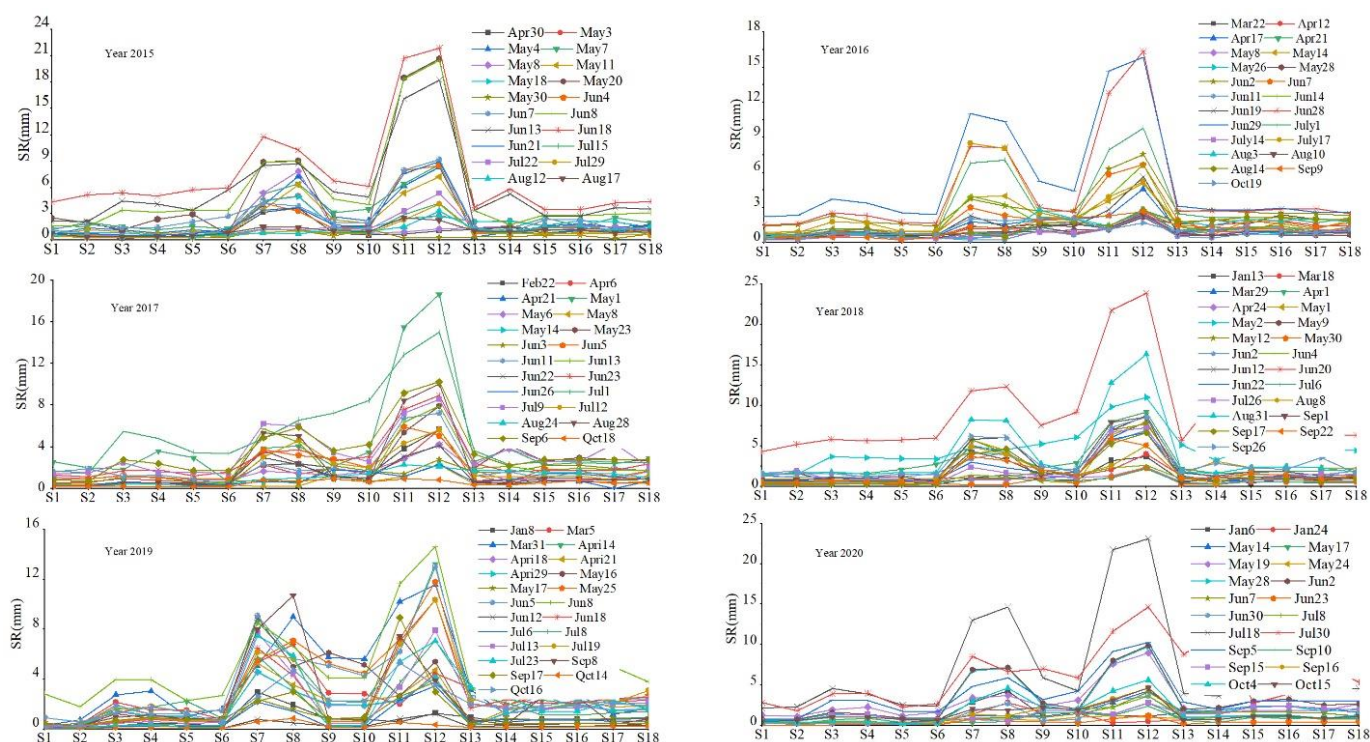


Figure 5. Plots surface runoffs of rainfall-runoff events in 2015–2020.

Among all the rainfall-runoff events, the mean SR generating from fallow land was 133.90 mm and ranked first because of the bare karst yellow soil without vegetation cover was more conducive to infiltration. The mean SR amount generated from cropland was 82.89 mm, which was much higher than other vegetation cover types. The mean SR of broadleaf forest, coniferous forest, mixed forest, orchard, and grassland were 25.88 mm, 17.37 mm, 21.56 mm, 37.37 mm, and 44.69 mm, respectively, which were 19.33%, 12.97%, 16.10%, 33.38%, and 27.65% of fallow land, respectively. The vegetation root system or dead fall of the plots with vegetation cover could well hold rainwater and reduce the surface runoff.

The mean RC of fallow, cropland, broad-leaved forest, coniferous forest, mixed forest, orchard, and grassland were 17.77%, 10.97%, 3.48%, 2.31%, 2.85%, 4.98%, and 6.01%, respectively. The RCs of fallow and cropland were also much higher than that of other forests and grasslands. The RC is strongly influenced by land use composition, and the forest land use displayed the most important control on the RC. There is a strong positive relationship between sediment yield and runoff coefficient (RC), which means more soil erosion when RC is higher [61].

The standard deviations of SR and RC of cropland and fallow floor were also much higher than other vegetation cover land floors, indicating their interval dispersions were much higher, and SR and RC of cropland and fallow floor vary considerably under different rainfall conditions.

(2) Runoff sediment loss characteristics

The runoff sediment concentration (RSC, $\text{kg}\cdot\text{m}^{-3}$) of all the 139 rainfall-runoff events in 2015–2020 are shown according to the eighteen runoff plots in Figure 6.

Based on the runoff sediment concentrations (RSC, $\text{kg}\cdot\text{m}^{-3}$), the sediment loss rates (SLR, $\text{t}\cdot\text{ha}^{-1}\cdot\text{a}^{-1}$) of different runoff plots was calculated. The RSC and SLR statistical parameters of the seven groups plots are listed in the following Table 3.

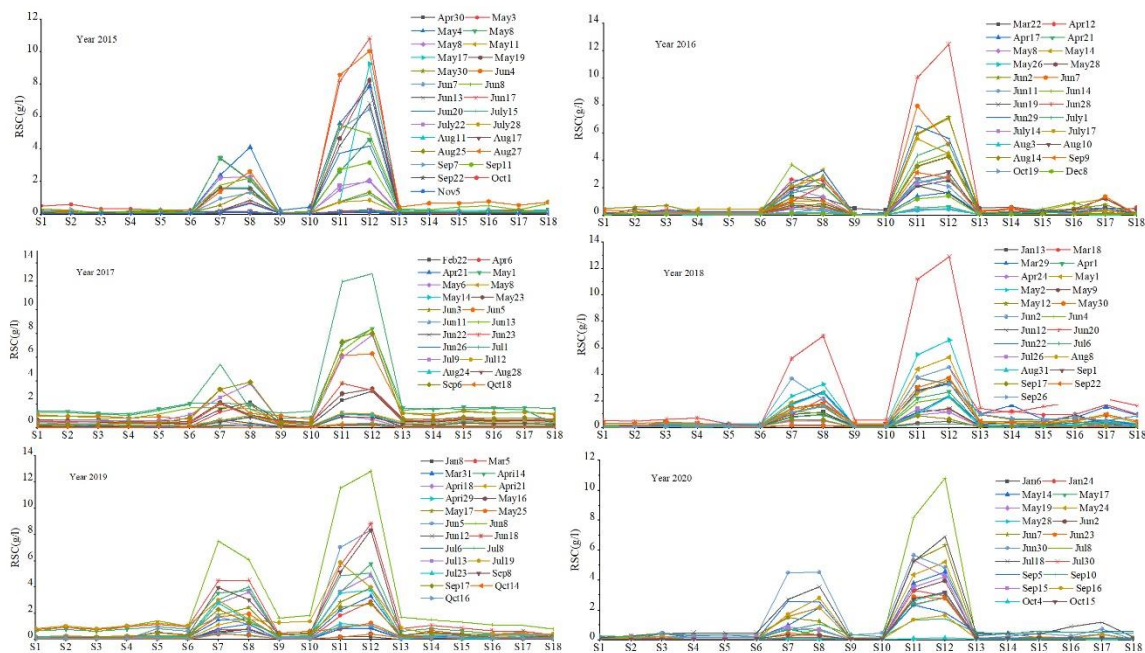


Figure 6. Runoff sediment concentrations of rainfall-runoff events in 2015–2020.

Table 3. The runoff sediment concentrations and sediment losses of runoff plots.

Plots	Vegetation Types	RSC ($\text{kg}\cdot\text{m}^{-3}$)		SLR ($\text{t}\cdot\text{ha}^{-1}\cdot\text{a}^{-1}$)	
		Mean	SD	Mean	SD
S1–S2	Broad-leaved forest	0.14	0.13	1.62	2.03
S3–S4	Coniferous forest	0.12	0.11	1.36	1.25
S5–S6	Coniferous & broad-leaved mixed forest	0.13	0.16	1.49	2.13
S7–S8	Cropland	1.39	0.35	12.64	6.76
S9–S10	Grassland	0.16	0.12	1.85	1.08
S11–S12	Fallow	3.32	0.41	23.49	9.26
S13–S18	Orchard	0.29	0.18	2.97	3.24

The mean RSC values ranged from $0.12 \text{ kg}\cdot\text{m}^{-3}$ (coniferous forest) to $3.32 \text{ kg}\cdot\text{m}^{-3}$ (fallow). RSC of fallow was the highest, which was significantly larger than that the other observed plots. RSC of cropland was $1.39 \text{ kg}\cdot\text{m}^{-3}$ and also much larger than other plots. The mean RSC values of broad-leaved forest, coniferous forest, mixed forest, orchard, and grassland were $0.14 \text{ kg}\cdot\text{m}^{-3}$, $0.12 \text{ kg}\cdot\text{m}^{-3}$, $0.13 \text{ kg}\cdot\text{m}^{-3}$, $0.29 \text{ kg}\cdot\text{m}^{-3}$, and $0.16 \text{ kg}\cdot\text{m}^{-3}$, respectively, which were 4.22%, 3.61%, 3.92%, 8.73% and 4.82% of the fallow land, respectively.

The mean SLR of fallow, cropland, broad-leaved forest, coniferous forest, mixed forest, orchard, and grassland were $23.49 \text{ t}\cdot\text{ha}^{-1}\cdot\text{a}^{-1}$, $12.64 \text{ t}\cdot\text{ha}^{-1}\cdot\text{a}^{-1}$, $1.62 \text{ t}\cdot\text{ha}^{-1}\cdot\text{a}^{-1}$, $1.36 \text{ t}\cdot\text{ha}^{-1}\cdot\text{a}^{-1}$, $1.49 \text{ t}\cdot\text{ha}^{-1}\cdot\text{a}^{-1}$, $2.97 \text{ t}\cdot\text{ha}^{-1}\cdot\text{a}^{-1}$, and $1.85 \text{ t}\cdot\text{ha}^{-1}\cdot\text{a}^{-1}$, respectively. The SLR values of fallow and cropland were also much higher than that of forests and grasslands. The mean SLR values of broad-leaved forest, coniferous forest, mixed forest, orchard, and grassland were 6.90%, 5.79%, 6.34%, 12.64%, and 7.88% of the fallow land, respectively. Therefore, the benefits of different forests and grasslands were very significant as shown in the RSC and SLR reductions, which reflect soil erosion mitigation.

The standard deviations of SCR and SLR of cropland and fallow floor were also much higher than other vegetation cover land floors, indicating the SR and RC of cropland and fallow floor vary considerably under different rainfall conditions.

3.3. SEM Analysis of the Effecting Factors

Direct and indirect relationships among precipitation (P , mm), 30-min maximum rainfall intensity (I_{30} , $\text{mm}\cdot\text{h}^{-1}$), rainfall erosivity R value (R , $\text{MJ}\cdot\text{mm}\cdot\text{ha}^{-1}\cdot\text{h}^{-1}$), surface runoff (SR , mm), antecedent soil water content (ASW , %), vegetation coverage (VC , %), runoff sediment concentration (RSC , $\text{kg}\cdot\text{m}^{-3}$), and sediments loss rate (SLR) were evaluated using structural equation modeling (SEM) (Figure 7).

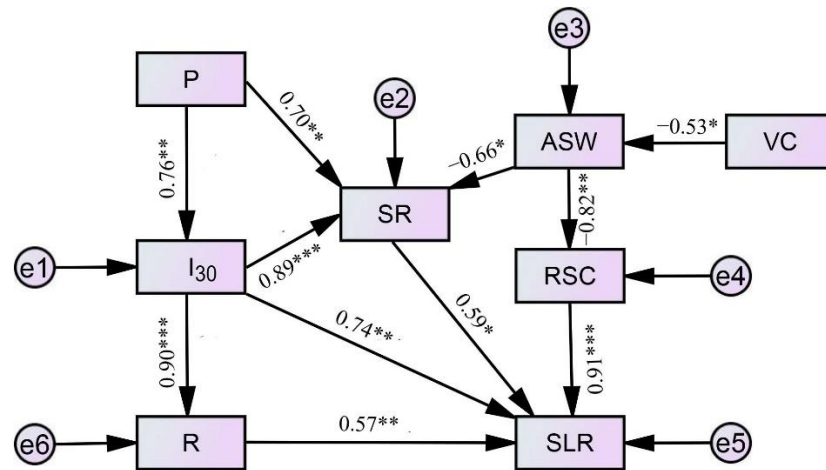


Figure 7. Structural equation model of direct and indirect relationships. Note: *** indicates the standardized path coefficient is significant at the level of 0.001; ** indicates it is significant at the level of 0.01; * indicates it is significant at the level of 0.05; e1–e6: denote the residual terms of the respective corresponding terms.

Relevant parameters for discriminating model fitness based on the model, $\chi^2/\text{df} = 2.166$, $p = 0.071 > (p > 0.05)$, were generated. Therefore, the null hypothesis was accepted. $\text{GFI} = 0.786$, $\text{NFI} = 0.713$, $\text{IFI} = 0.788$, $\text{CFI} = 0.813$. All were greater than 0.7, and the model was acceptable. $\text{RMSEA} = 0.033 (< 0.05)$, which was also acceptable. SR generation at the plot scale was substantially linked directly with I_{30} , and VC and ASW had negative direction inferences with SR and RSC according to SEM analysis. The VC and ASW resulted in the highest indirect impacts on SLR .

4. Discussion

4.1. Characteristics of Sediment Loss in Karst Region

China's southwestern karst region is one of the world's largest continuous karst terrain areas exposed to a subtropical climate. The sediment loss rate (SLR) given by different researchers often vary widely. Measurements at the hydrological stations of Guilin and Fuyang in Guangxi found the river sand content was $0.06\text{--}0.10 \text{ kg}\cdot\text{m}^{-3}$, and the suspended mass erosion modulus was $0.6\text{--}0.7 \text{ t}\cdot\text{ha}^{-1}\cdot\text{a}^{-1}$ [62]. The monitoring of major rivers in the Guizhou Mountains revealed the average sand transport modulus of the rivers was $3.22 \text{ t}\cdot\text{ha}^{-1}\cdot\text{a}^{-1}$ with the highest being $10.47 \text{ t}\cdot\text{ha}^{-1}\cdot\text{a}^{-1}$ (Wudu River) and the lowest being $0.56 \text{ t}\cdot\text{ha}^{-1}\cdot\text{a}^{-1}$ (Zhanjiang River) [63]. The average erosion modulus was $3.88 \text{ t}\cdot\text{ha}^{-1}\cdot\text{a}^{-1}$, and the maximum erosion modulus is $13.00 \text{ t}\cdot\text{ha}^{-1}\cdot\text{a}^{-1}$ in Wenshan, Yunnan [64]. Based on the remote sensing interpretation and typical sample area information, the area of stone desertification with plants above $5.00\text{--}25.00 \text{ t}\cdot\text{ha}^{-1}\cdot\text{a}^{-1}$ erosion modulus of karst in Guizhou accounted for 7.5%, and the area of stone desertification with $25.00\text{--}50.00 \text{ t}\cdot\text{ha}^{-1}\cdot\text{a}^{-1}$ erosion modulus accounted for 20.4% of the province [8]. By applying the modified US universal soil loss equation (RUSLE) with the support of GIS remote sensing technology, the average soil erosion modulus was calculated at $0.29 \text{ t}\cdot\text{ha}^{-1}\cdot\text{a}^{-1}$ in the Cat Jump River watershed in Guizhou Province [65]. The average erosion of forest and grassland was $1.13 \text{ t}\cdot\text{ha}^{-1}\cdot\text{a}^{-1}$, the average erosion of gently sloping crop land was $5.66 \text{ t}\cdot\text{ha}^{-1}\cdot\text{a}^{-1}$, and the average erosion of steeply sloping crop land was $22.65 \text{ t}\cdot\text{ha}^{-1}\cdot\text{a}^{-1}$ [66], which is comparable to the actual

monitoring result in this study. In general, in the early erosion stage after forest destruction, soil erosion intensity is usually decreasing sharply with the exhaustion of nourishing erodible soils. The soil erosion intensity often varies greatly depending on the study area, observation scale, and method.

4.2. Factors Influencing on Surface Runoff and Sediment Loss

Both climate change and human activity have a significant impact on surface runoff [67–69]. Global compilations of data reveal soil loss rates from agricultural systems are significantly higher than those from areas with natural vegetation [11]. Precipitation changes (72% of the reduction in water discharge in the Yangtze River) and human activities (86% of the reduction in sediment discharge) are also major contributors [70]. In this paper, under the same natural rainfall condition, the mean SR of broadleaf forest, coniferous forest, mixed forest, orchard, and grassland were 19.33%, 12.97%, 16.10%, 33.38%, and 27.65% of fallow land, respectively, while the mean SR of cropland was 61.91%. Because of the increased human activities, the mean SR of cropland increased obviously, which was 4.47 times the coniferous forest, and 3.20, 3.84, and 2.24 times the broad-leaved forest, mixed forest, and orchard, respectively.

The mean SLR of fallow, cropland, broad-leaved forest, coniferous forest, mixed forest, orchard, and grassland were $23.49 \text{ t}\cdot\text{ha}^{-1}\cdot\text{a}^{-1}$, $12.641 \text{ t}\cdot\text{ha}^{-1}\cdot\text{a}^{-1}$, $1.62 \text{ t}\cdot\text{ha}^{-1}\cdot\text{a}^{-1}$, $1.36 \text{ t}\cdot\text{ha}^{-1}\cdot\text{a}^{-1}$, $1.49 \text{ t}\cdot\text{ha}^{-1}\cdot\text{a}^{-1}$, $2.97 \text{ t}\cdot\text{ha}^{-1}\cdot\text{a}^{-1}$, and $1.85 \text{ t}\cdot\text{ha}^{-1}\cdot\text{a}^{-1}$, respectively. Because of the increased human activities, the mean SLR of cropland were 7.80, 9.29, 8.48, 4.26, and 6.83 times of the broad-leaved forest, coniferous forest, mixed forest, orchard, and grassland, respectively.

Structural equation modeling (SEM) analysis showed the relevant parameters for discriminating model fitness was acceptable. SR generation at the plot scale exhibits a significant direct positive influence by I_{30} and direct negative influence by ASW, while VC and ASW show the highest indirect impact on SLR, which were in agreement with the results reported by Cammeraat (2004) [71].

5. Conclusions

The objective of this paper is to observe and comparatively study the runoff generation and sediment loss on different forest and other land floors at a karst yellow soil region in Southwest China. Based on long-term (2015–2020), six years natural rainfall events data of 18 runoff plots, the results of the statistical analysis and structural equation modeling (SEM) analysis can be summarized as the following:

- (1) The average annual rainfall of study area in 2015–2020 was 1207.7 mm and concentrated in April–October; combined with the high susceptibility to erosion of karst yellow soil, accelerated soil erosion threatens human societies. There were 139 rainfall-runoff events occurring in 2015–2020, mainly moderate rain and heavy rain events. Heavy rain contributed the most to the total rainfall erosivity R value because of its high frequency and long duration.
- (2) The observation results of 18 runoff plots in Yangjichong soil and water conservation monitoring station from 2015 to 2020 indicated under the same rain conditions, different water conservation forest and different plating patterns had greater influence on surface runoff generation and sediment loss. Under the same natural rainfall conditions, the mean SR generating from fallow land and cropland were 133.90 mm and 82.89 mm, respectively, which were much higher than other vegetation cover types. The mean SR of broadleaf forest, coniferous forest, mixed forest, orchard, and grassland were 17.37 mm, 25.88 mm, 21.56 mm, 37.37 mm, and 44.69 mm, respectively, which were 19.33%, 12.97%, 16.10%, 33.38%, and 27.65% of fallow land, respectively. The vegetation root system or dead fall of the plots with vegetation cover could well hold rainwater and reduce the surface runoff.
- (3) The highest mean RSC value was $3.32 \text{ kg}\cdot\text{m}^{-3}$ of fallow, which was significantly larger than that observed for most other plots. The RSC value of cropland was

1.39 kg·m⁻³ and much larger than other plots. The mean RSC value of grassland was the lowest, indicating the grassland could maintain the karst yellow soil well. The mean SLR values of fallow and cropland were also much higher than that of other forests and grasslands. The standard deviations of SCR and SLR indicated SCR and SLR of cropland and fallow floor also vary considerably under different rainfall conditions.

- (4) Structural equation modeling analysis showed the relevant parameters for discriminating model fitness was acceptable. SR generation at the plot scale was substantial linked directly with I₃₀. The VC and ASW resulted in the highest indirect impact on SLR.

This study discussed the basic soil erosion external dynamics parameters for the erosion forecasting model in the karst yellow soil region in Southwest China. On this basis, the erosive rainfall and sediment production analysis of different vegetation cover land floors is of great value for soil erosion forecasting in the karst yellow soil region. Our study suggests improving vegetation cover is a reasonable land use strategy to effectively manage sustainable land use in karst regions. The measuring of SR reduction and RSC reduction effects according to different forests and grassland floors can also provide scientific guidance for regional agricultural production.

Author Contributions: Conceptualization, R.P., H.D., R.L. and Y.L.; methodology, R.P., H.D., O.D., Y.L. and G.Y.; software, R.P., H.D., Y.L. and G.Y.; validation, Y.L. and G.Y.; formal analysis, R.P., H.D., R.L. and Y.L.; investigation, O.D., R.P. and Y.L.; resources, O.D.; data curation, R.P., H.D., R.L. and Y.L.; writing—original draft preparation, R.P., H.D. and O.D.; writing—review and editing, Y.L. and R.P.; visualization, O.D. and G.Y.; supervision, Y.L.; project administration, Y.L.; funding acquisition, Y.L., O.D. and G.Y. All authors have read and agreed to the published version of the manuscript.

Funding: This work was funded by the Science and Technology Program of Guizhou Province (2020 1Z031); the Science and Technology Program of Guizhou Province (2019 1222); the Joint Fund of the National Natural Science Foundation of China and the Karst Science Research Center of Guizhou Province (Grant No. U1812401); the open project of Ecological Security and Protection Key Laboratory of Sichuan Province (ESP201304); the Science and Technology Program of Guizhou Province (2019 1218).

Institutional Review Board Statement: Not applicable.

Informed Consent Statement: Not applicable.

Data Availability Statement: All data in this study were correctly referenced.

Conflicts of Interest: The authors declare no conflict of interest.

References

1. Yuan, D.; Jiang, Y.; Shen, L.; Pu, J.; Xiao, Q. *Modern Karstology*; Science Press: Beijing, China, 2016. (In Chinese)
2. Song, T.Q.; Peng, W.X.; Du, H.; Wang, K.L.; Zeng, F.P. Occurrence, spatial-temporal dynamics and regulation strategies of karst rocky desertification in south-west China. *Acta Ecol. Sin.* **2014**, *34*, 5328–5341.
3. Hartmann, A.; Goldscheider, N.; Wagener, T.; Lange, J.; Weiler, M. Karst water resources in a changing world: Review of hydrological modeling approaches. *Rev. Geophys.* **2015**, *52*, 218–242. [[CrossRef](#)]
4. Wang, S.; Yan, Y.; Fua, Z.; Chen, H. Rainfall-runoff characteristics and their threshold behaviors on a karst hillslope in a peak-cluster depression region. *J. Hydrol.* **2022**, *605*, 127370. [[CrossRef](#)]
5. Sweeting, M.M. *Karst in China: Its Geomorphology and Environment*; Springer: Berlin/Heidelberg, Germany, 1995; pp. 1–5.
6. Ford, D.C.; Williams, P.W. *Karst Hydrology and Geomorphology*; Chapman & Hall: London, UK, 2007; pp. 1–5.
7. Wang, S.; Fu, Z.; Chen, H.; Nie, Y.; Xu, Q. Mechanisms of surface and subsurface runoff generation in subtropical soil epi-karst systems: Implications of rainfall simulation experiments on karst slope. *J. Hydrol.* **2020**, *580*, 124370. [[CrossRef](#)]
8. Xiong, K.N. *Remote Sensing-GIS Typical Study of Karst Desertification—The Example of Guizhou Province*; Geological Press: Beijing, China, 2002; pp. 1–10. (In Chinese)
9. Wang, S.J.; Li, Y.B.; Li, R.L. Karst Rocky Desertification: Formation Background, Evolution and Comprehensive Taming. *Quat. Sci.* **2003**, *23*, 657–666. (In Chinese)
10. Wilcox, B.P.; Taucer, P.I.; Munster, C.L.; Owens, M.K.; Mohanty, B.P.; Sorenson, J.R.; Bazan, R. Subsurface stormflow is important in semiarid karst shrub lands. *Geophys. Res. Lett.* **2008**, *35*, L10403. [[CrossRef](#)]

11. Anache, J.A.A.; Wendland, E.C.; Oliveira, P.T.S.; Flanagan, D.C.; Nearing, M.A. Runoff and soil erosion plot-scale studies under natural rainfall: A meta-analysis of the Brazilian experience. *Catena* **2017**, *152*, 29–39.
12. Tsozué, D.; Nghonda, J.P.; Mekem, D.L. Impact of land management system on crop yields and soil fertility in Cameroon. *Solid Earth* **2015**, *6*, 1087–1101. [[CrossRef](#)]
13. Nysse, J.; Frankl, A.; Zenebe, A.; Poesen, J.; Deckers, J. Environmental conservation for food production and sustainable livelihood in Tropical Africa. *Land. Degrad. Dev.* **2015**, *26*, 629–631. [[CrossRef](#)]
14. Tesfaye, M.A.; Bravo-Oviedo, A.; Bravo, F.; Kidane, B.; Bekele, K.; Sertse, D. Selection of tree species and soil management for simultaneous fuelwood production and soil rehabilitation in the Ethiopian central highlands. *Land Degrad. Dev.* **2015**, *26*, 665–679. [[CrossRef](#)]
15. Oliveira, S.P.; Lacerda, N.B.; Blum, S.C.; Escobar, M.E.O.; Oliveira, T.S. Organic carbon and nitrogen stocks in soils of Northeastern Brazil converted to irrigated agriculture. *Land. Degrad. Dev.* **2015**, *26*, 9–21. [[CrossRef](#)]
16. Oliveira, P.T.S.; Nearing, M.A.; Wendland, E. Orders of magnitude increase in soil erosion associated with land use change from native to cultivated vegetation in a Brazilian savannah environment. *Earth Surf. Process. Landf.* **2015**, *40*, 1524–1532. [[CrossRef](#)]
17. García-Ruiz, J.M.; Beguería, S.; Nadal-Romero, E.; González-Hidalgo, J.C.; Lana-Renault, N.; Sanjuán, Y. A meta-analysis of soil erosion rates across the world. *Geomorphology* **2015**, *239*, 160–173. [[CrossRef](#)]
18. Guo, Q.; Hao, Y.; Liu, B. Rates of soil erosion in China: A study based on runoff plot data. *Catena* **2015**, *124*, 68–76. [[CrossRef](#)]
19. Wischmeier, W.H.; Smith, D.D. Rainfall energy and its relationship to soil loss. *EOS Trans. Am. Geophys. Union* **1958**, *39*, 285–291. [[CrossRef](#)]
20. Hartanto, H.; Prabhub, R.; Widayatc, A.S.E.; Asdak, C. Factors affecting runoff and soil erosion: Plot-level soil loss monitoring for assessing sustainability of forest management. *For. Ecol. Manag.* **2003**, *180*, 361–374. [[CrossRef](#)]
21. Li, X.-Y.; Contreras, S.; Solé-Benet, A.; Cantón, Y.; Domingo, F.; Lázaro, R.; Lin, H.; van Wesemael, B.; Puigdefàbregas, J. Controls of infiltration—runoff processes in Mediterranean karst rangelands in SE Spain. *Catena* **2011**, *86*, 98–109. [[CrossRef](#)]
22. Kim, J.K.; Onda, Y.; Kim, M.S.; Yang, D.Y. Plot-scale study of surface runoff on well-covered forest floors under different canopy species. *Quat. Int.* **2014**, *344*, 75. [[CrossRef](#)]
23. Miller, M.F. Waste through soil erosion. *J. Am. Soc. Agron.* **1926**, *18*, 153–160. [[CrossRef](#)]
24. Wischmeier, W.H.; Smith, D.D. *Predicting Rainfall Erosion Losses—A Guide to Conservation Planning*; Agriculture Handbook; US Department of Agriculture: Washington, DC, USA, 1978.
25. Ji, Q.-F.; Zhang, X.-Q.; Zhang, K.-L.; Yang, Y.; Yang, G.-X.; Gu, Z.-K. Runoff and sediment characteristics of slope land in karst areas of Guizhou Province. *Res. Soil Water Conserv.* **2012**, *19*, 1–5. (In Chinese)
26. Zhou, Y.; Wei, T.-X.; Xie, J.-Q.; Shi, X.; Ge, G.-B.; Dong, Z.; Cheng, Z.-Q. Different types of vegetation cover and water conservation benefits. *J. Soil Water Conserv.* **2012**, *19*, 12–16. (In Chinese)
27. Lv, Y.-J.; Peng, X.-H.; Gao, L.; Zhang, Z.-B. Characteristics of runoff and soil loss and their influential factors on sloping land in red soil hilly region. *J. Soil Water Conserv.* **2014**, *28*, 19–23, 51. (In Chinese)
28. Wischmeier, W.H.; Smith, D.D. *Predicting Rainfall Erosion Losses from Cropland East of the Rocky Mountains*; Agriculture Handbook; US Department of Agriculture: Washington, DC, USA, 1965.
29. Renard, K.G.; Foster, G.R.; Weesies, G.A.; McCool, D.K.; Yoder, D.C. *Predicting Soil Erosion by Water: A Guide to Conservation Planning with the Revised Universal Soil Loss Equation (RUSLE)*; Agriculture Handbook; USDA: Washington, DC, USA, 1997; p. 703.
30. Goblin, A.; Jones, R.; Kirkby, M.; Campling, P.; Govers, G.; Kosmas, C.; Gentile, R.A. Indicators for pan-European assessment and monitoring of soil erosion by water. *Environ. Sci. Pol.* **2004**, *7*, 25–38. [[CrossRef](#)]
31. Cerdan, O.; Govers, G.; Le Bissonnais, Y.; Van Oost, K.; Poesen, J.; Saby, N.; Gobin, A.; Vacca, A.; Quinton, J.; Auerswald, K.; et al. Rates and spatial variations of soil erosion in Europe: A study based on erosion plot data. *Geomorphology* **2010**, *122*, 167–177. [[CrossRef](#)]
32. Roose, E.J. Use of the Universal Soil Loss Equation to Predict Erosion in West Africa. In *Proceedings of the Soil Erosion: Prediction and Control*, West Lafayette, IN, USA, 23–28 May 1999.
33. Stocking, M.A. Rates of erosion and sediment yield in the African environment. In *Challenges in African Hydrology and Water Resources*; Walling, D.E., Foster, S.S.D., Wurzel, P., Eds.; International Association of Scientific Hydrology (IASH-AIHS): Wallingford, UK, 1984; Volume 144, pp. 285–295.
34. Lu, H.; Prosser, I.P.; Moran, C.J.; Gallant, J.C.; Priestley, G.; Stevenson, J.G. Predicting sheet wash and rill erosion over the Australian continent. *Soil Res.* **2003**, *41*, 1037–1062. [[CrossRef](#)]
35. Liu, Y.B.; Xie, Y.; Zhang, K.L. *Soil Erosion Prediction Model*; Science Press: Beijing, China, 2001. (In Chinese)
36. Huang, C.B.; Liu, Y.H.; Qin, W.M.; Wei, S.H.; Huang, D.; Li, B.P. Study on the water and soil erosion rules during the three types of vegetation recovery process. *J. Nanjing For. Univ.* **2010**, *34*, 59–64. (In Chinese)
37. Guo, S.Y.; Li, Z.G. Development and achievements of soil and water conservation monitoring in China. *Sci. Soil Water Conserv.* **2009**, *7*, 19–24. (In Chinese)
38. Zhang, X.K.; Xu, J.H.; Lu, X.Q.; Deng, Y.J.; Gao, D.W. A study on the soil loss equation in Heilongjiang Province. *Bull. Soil Water Conserv.* **1992**, *12*, 1–9. (In Chinese)
39. Jiang, Z.S.; Wang, Z.Q.; Liu, Z. Quantitative Study on Spatial Variation of Soil Erosion in a Small Watershed in the Loess Hilly Region. *J. Soil Eros. Soil Conserv.* **1996**, *2*, 1–9. (In Chinese)

40. Cai, Q.G.; Lu, Z.X.; Wang, G.P. Process-based soil erosion and sediment yield model in a small basin in the hilly loess region. *Acta Geogr. Sin.* **1996**, *51*, 108–117. (In Chinese)
41. Liu, W.; Li, Z.; Zhu, J.; Xu, C.; Xu, X. Dominant factors controlling runoff coefficients in karst watersheds. *J. Hydrol.* **2020**, *590*, 125486. [[CrossRef](#)]
42. Dieterich, M. Dynamics of a biotic parameters, solute removal and sediment retention in summer-dry headwater streams of western Oregon. *Hydrobiologia* **1998**, *379*, 1–15. [[CrossRef](#)]
43. Duan, L.; Huang, M.; Zhang, L. Differences in hydrological responses for different vegetation types on a steep slope on the Loess Plateau, China. *J. Hydrol.* **2016**, *537*, 356–366. [[CrossRef](#)]
44. Kou, X.Y.; Huang, J.; Jiang, X.B.; Xiang, J.P.; Jin, P.W.; Wang, S.W. Effects of Rainfall on Runoff and Sediment Under Different Underlying Surfaces of Runoff Plots. *Bull. Soil Water Conserv.* **2017**, *37*, 27–31.
45. Zhao, Q.; Zhang, Y.; Xu, S.; Ji, X.; Wang, S.; Ding, S. Relationships between riparian vegetation pattern and the hydraulic characteristics of upslope runoff. *Sustainability* **2019**, *11*, 2966. [[CrossRef](#)]
46. Hou, G.R.; Bi, H.X.; Huo, Y.M.; Wei, X.; Zhu, Y.; Wang, X.; Liao, W. Determining the optimal vegetation coverage for controlling soil erosion in Cynodon dactylon grassland in North China. *J. Clean. Prod.* **2020**, *244*, 118771. [[CrossRef](#)]
47. Dai, H.L.; Yuan, S.; Zhang, K.L.; Zhu, Q. Spatial and temporal variation of rainfall erosion force in Guizhou Province. *Res. Soil Water Conserv.* **2013**, *20*, 37–41. (In Chinese)
48. Li, Y.Q.; Deng, O.; Yang, G.B.; Fang, Q.B. Distribution Characteristics of Rainfall erosivity R Value in Yellow Soil Area of Central Guizhou Karst Mountainous Region. *Bull. Soil Water Conserv.* **2021**, *41*, 31–49. (In Chinese)
49. Cai, X.F. Influencing Factors Analysis and Numerical Simulation on Erosion of Yellow Soil in Southwest Karst Area, China. Master's Thesis, Guizhou Normal University, Guiyang, China, 2009. (In Chinese).
50. Ping, Y.; Kangning, X.; Hengsong, W.; Jin, L.; Yang, L. Progress of Study on Soil and Water Loss and Soil and Water Conservation of Karst Region. *Soil Water Conserv. China* **2017**, *1*, 54–59. (In Chinese)
51. Yang, Q.; Yang, G.B.; Zhao, Q.; Dai, L. Characteristics of runoff sediment yield on slopes under different rainfall and vegetation cover in karst areas. *Bull. Soil Water Conserv.* **2020**, *40*, 9–16. (In Chinese)
52. Zhang, W.Y.; Wang, B.T.; Yang, G.X.; Zhang, K.L. Erosive Rainfall and Characteristics Analysis of Sediment Yield on Yellow Soil Area in Karst Mountainous. *Ecol. Environ. Sci.* **2014**, *23*, 1776–1782. (In Chinese)
53. Liang, W.L.; Chan, M.C. Spatial and temporal variations in the effects of soil depth and topographic wetness index of bedrock topography on subsurface saturation generation in a steep natural forested headwater catchment. *J. Hydrol.* **2017**, *546*, 405–418. [[CrossRef](#)]
54. Wischmeir, W.H. Estimating the Loss Equation's Cover and Management Factor for Undisturbed Areas. In *Proceedings of Sediment Yield Workshop*; U.S. Department of Agriculture Sedimentation Laboratory: Oxford, MS, USA, 1972.
55. Grace, J.B. The factors controlling species density in herbaceous plant communities: An assessment. *Perspect. Plant Ecol. Evol. Syst.* **1999**, *2*, 1–28. [[CrossRef](#)]
56. Grace, J.B.; Anderson, T.M.; Smith, M.D.; Seabloom, E.; Andelman, S.J.; Meche, G.; Weiher, E.; Allain, L.K.; Jutila, H.; Sankaran, M.; et al. Does species diversity limit productivity in natural grassland communities? *Ecol. Lett.* **2007**, *10*, 680–689. [[CrossRef](#)] [[PubMed](#)]
57. Riseng, C.M.; Wiley, M.J.; Black, R.W.; Munn, D.M. Impacts of agricultural land use on biological integrity: A causal analysis. *Ecol. Appl.* **2011**, *21*, 3128–3146. [[CrossRef](#)]
58. Matías, L.; Castro, J.; Zamora, R. Effect of Simulated Climate Change on Soil Respiration in a Mediterranean-Type Ecosystem: Rainfall and Habitat Type are More Important than Temperature or the Soil Carbon Pool. *Ecosystems* **2012**, *15*, 299–310. [[CrossRef](#)]
59. Mcleod, E.S.; Banerjee, E.W. Bork. Structural equation modeling reveals complex relationships in mixed forage swards. *Crop Prot.* **2015**, *78*, 106–113. [[CrossRef](#)]
60. GB T 20486—2017; Inspection and Quarantine of the People's Republic of China. Surface Rainfall Grade in River Basin. China Standards Press: Beijing, China, 2017.
61. Parsons, A.J.; Brazier, R.E.; Wainwright, J.; Powell, D.M. Scale relationships in hillslope runoff and erosion. *Earth Surf. Processes Landf.* **2006**, *31*, 1384–1393. [[CrossRef](#)]
62. Chai, Z.X. Soil erosion in karst area of Guangxi autonomous region. *Mt. Res.* **1989**, *7*, 255–259.
63. Zhu, A.G.; Lin, C.H. *The Synthetical Study on Elements of Loss of Water and Soil in Mountain Area*; Guizhou Scientific and Technological Pressing: Guiyang, China, 1995; pp. 48–60.
64. Chen, X.P. Research on characteristics of soil erosion in karst mountainous region environment. *J. Soil Eros. Soil Water Conserv.* **1997**, *3*, 31–36.
65. Xu, Y.-Q.; Shao, X.-M. Estimation of soil erosion supported by GIS and RUSLE: A Study of Mao-tiao river watershed, Guizhou Province. *J. Beijing For. Univ.* **2006**, *28*, 67–71.
66. Zhiwei, Z.; Liwa, F.; Hong, Z. Study on soil erosion of different degrees in karst region by using Cesium-137 technique. *J. Mt. Sci.* **2007**, *25*, 302–308.
67. Zhan, C.S.; Jiang, S.S.; Sun, F.B.; Jia, Y.W.; Yue, W.F.; Niu, C.W. Quantitative contribution of climate change and human activities to runoff changes in the Wei river basin, China. *Hydrol. Earth Syst. Sci.* **2014**, *11*, 2149–2175. [[CrossRef](#)]
68. Wei, L.; Dan, B.; Wang, F.; Fu, B.; Yan, J.; Shuai, W. Quantifying the impacts of climate change and ecological restoration on streamflow changes based on a budyko hydrological model in China's loess plateau. *Water Resour. Res.* **2015**, *51*, 6500–6519.

69. Xu, Y.; Wang, S.; Bai, X.; Shu, D.; Tian, Y. Runoff response to climate change and human activities in a typical karst watershed, SW China. *PLoS ONE* **2018**, *13*, e0193073. [[CrossRef](#)] [[PubMed](#)]
70. Zhao, Y.; Zou, X.; Gao, J.; Xu, X.; Wang, C.; Tang, D. Quantifying the anthropogenic and climatic contributions to changes in water discharge and sediment load into the sea: A case study of the Yangtze river, China. *Sci. Total Environ.* **2015**, *536*, 803–812. [[CrossRef](#)]
71. Cammeraat, E.L.H. Scale dependent thresholds in hydrological and erosion response of a semi-arid catchment in southeast Spain. *Agric. Ecosyst. Environ.* **2004**, *104*, 317–332. [[CrossRef](#)]

Disclaimer/Publisher's Note: The statements, opinions and data contained in all publications are solely those of the individual author(s) and contributor(s) and not of MDPI and/or the editor(s). MDPI and/or the editor(s) disclaim responsibility for any injury to people or property resulting from any ideas, methods, instructions or products referred to in the content.